Band rearrangement through the 2D-Dirac equation: Comparing the APS and the chiral bag boundary conditions

T. Iwai [a,*], B. Zhilinskii [b]

[a] *Kyoto University, 606-8501 Kyoto, Japan*
[b] *Université du Littoral Côte d'Opale, Dunkerque, France*

Abstract

The Dirac equation on a two-disk is studied under the chiral bag boundary condition, where the mass is treated as a parameter ranging over all real numbers. The eigenvalues as functions of the parameter are compared with those obtained under the APS boundary condition studied in a previous paper of authors (Iwai and Zhilinskii, 2015). Discrete symmetry (or pseudo-symmetry) of the boundary condition as well as the Hamiltonian is studied to explain the difference between the patterns of eigenvalues under the chiral bag and the APS boundary conditions. The spectral flow for a one-parameter family of operators is the net number of eigenvalues passing through zero in the positive direction as the parameter runs. It was demonstrated in the previous paper that the spectral flow is useful to understand the characteristic of eigenvalue pattern of the Dirac equation with the APS boundary condition. However, to capture the feature of eigenvalue pattern under the chiral bag boundary condition, one needs to introduce an extended notion of spectral flow. The eigenvalue patterns under the both boundary conditions are compared with a semi-quantum description of energy-band rearrangement.

* Corresponding author.
  E-mail addresses: iwai.toshihiro.63u@st.kyoto-u.ac.jp (T. Iwai), zhilin@univ-littoral.fr (B. Zhilinskii).

1. Introduction

This article is a sequel to a previous one [10]. In [10], the Dirac equation on a two-disk was treated under the APS (Atiyah–Patodi–Singer [2]) boundary condition, where the APS boundary condition requires that the boundary values of eigenstates should belong to the subspace of eigenstates associated with positive or negative eigenvalues for a chosen boundary operator. The spectral flow, which is defined for a generic one-parameter family of operators to be the net number of eigenvalues passing through zero in the positive direction as the parameter runs, is useful for the understanding of the pattern of eigenvalues as functions of the parameter. One of results of the previous article is that the spectral flow of a one-parameter family of the Dirac equation with the APS boundary condition is ± 1, depending on whether the sign of the total angular momentum eigenvalue j is positive or negative. A question arises as to whether the spectral flow is still useful for the description of the feature in the pattern of eigenvalues under another boundary condition. It will be shown that for the chiral bag boundary condition the notion of spectral flow is not applicable, since the passing through zero has no qualitative meaning for eigenvalues obtained under the chiral bag boundary condition. However, an answer to the above question will be possible if the notion of spectral flow is extended. Difference between the patterns of eigenvalues under the APS and the chiral boundary conditions can be explained by means of discrete symmetries (or pseudo-symmetries).

A further question is as to whether one can find a characteristic of band rearrangement independently of the choice of boundary conditions. This question comes from interest in the correspondence between a full quantum and a semi-quantum models. Semi-quantum models have been employed to study qualitative structure of energy bands in isolated molecules, in which the splitting of variables into two subclasses, "slow variables" and "fast variables", is assumed according to low- and high-energy excitation, and the slow and the fast variables are treated as classical and quantum ones, respectively. As long as a finite number of quantum levels are concerned, the Hamiltonian for the total system is described as a Hermitian matrix defined on a base manifold which is chosen on physical grounds. If the rotational variables are treated as classical ones, a chosen manifold is a two-sphere, which is a co-adjoint orbit of $SO(3)$ [5,11,12].

With each of disjoint eigenvalues viewed as functions on the two-sphere, is associated a complex line-bundle, which is characterized by a Chern number [5,7]. To model the band rearrangements, some control parameters are introduced into the Hamiltonian. Then, the band rearrangement is associated with a change in the Chern number accompanying the variation in the parameters. The delta-Chern was introduced in [8] to describe a change in the Chern number against the control parameters. The previous paper [10] shows that the spectral flow for the Dirac equation with the APS boundary condition naturally corresponds to the delta-Chern for a corresponding semi-quantum model. Rephrased from the viewpoint of the correspondence, a purpose of this article is to examine whether a choice of boundary condition affects the understanding of the correspondence between the full quantum and the semi-quantum models or not.

The organization of this article is as follows: Section 2 contains the setting up for solving the Dirac equation by using the method of separation of variables. Feasible solutions are given in terms of Bessel and modified Bessel functions in the radial variable as well as exponentials in the angular variable. Boundary conditions are treated in Section 3, in which the APS and the chiral bag boundary conditions are reviewed in a generic form. Section 4 includes analysis of eigenstates of the 2D-Dirac equation under the chiral bag boundary condition. Regular and edge states are found. They are described in terms of Bessel and modified Bessel functions, respectively, in the radial variable. Of particular interest are critical states, which are viewed as transient states

between regular and edge states. In Section 5, transition between regular and edge states through critical states is shown to occur indeed on the level of eigenvalues as well as eigenstates. The transition was not observed in the eigenvalues under the APS boundary condition [10], where the edge state persists for all the control parameter values except at a particular value only, at which the edge state changes into a zero mode. Section 6 deals with discrete symmetries (or pseudo-symmetries), which are used to explain the pattern of eigenvalues as functions of the parameter for both the chiral bag and the APS boundary conditions. In Section 7, an extended spectral flow is introduced to characterize the pattern of eigenvalues for the chiral bag boundary condition, which will be associated with the transition between regular and edge states. Section 8 deals with a corresponding semi-quantum system in order to characterize the band rearrangements in the semi-quantum model from a viewpoint other than that in [9,10] and thereby to compare with the extended or usual spectral flow. Section 9 contains concluding remarks.

2. Setting up

We make a brief review of the Dirac equation on a disk in $\mathbb{R}^2$ from [10]. The Dirac Hamiltonian on $\mathbb{R}^2$ is given by

$$
H_t = -i \sum_{k=1}^{2} \sigma_k \frac{\partial}{\partial q_k} + t\sigma_3 = \begin{pmatrix} t & -i\dfrac{\partial}{\partial q_1} - \dfrac{\partial}{\partial q_2} \\ -i\dfrac{\partial}{\partial q_1} + \dfrac{\partial}{\partial q_2} & -t \end{pmatrix},
\tag{1}
$$

where σ_k are the Pauli matrices. Let

$$
D(e^{i\tau}) := e^{-i\tau\sigma_3/2} = \begin{pmatrix} e^{-i\tau/2} & 0 \\ 0 & e^{i\tau/2} \end{pmatrix}, \qquad R(\tau) := \begin{pmatrix} \cos\tau & -\sin\tau \\ \sin\tau & \cos\tau \end{pmatrix}, \qquad \tau \in \mathbb{R}.
\tag{2}
$$

Then, the $U(1)$ action U_τ on the two-component spinor Φ on $\mathbb{R}^2$ is defined to be

$$
U_\tau \Phi = D(e^{i\tau}) \Phi \circ R(-\tau).
\tag{3}
$$

As is straightforwardly verified, the $U(1)$ symmetry of the H_t is described as

$$
U_\tau H_t U_\tau^{-1} = H_t.
\tag{4}
$$

The infinitesimal generator J of U_τ is called the (spin–orbital) angular momentum operator, which is determined through $U_\tau = \exp(-i\tau J)$ and expressed as

$$
J = \frac{1}{2}\sigma_3 + i\mathbb{1}\left(q_2 \frac{\partial}{\partial q_1} - q_1 \frac{\partial}{\partial q_2}\right),
\tag{5}
$$

where $\mathbb{1}$ denotes the 2×2 identity matrix.

In terms of the polar coordinates (r, θ), the Hamiltonian H_t and the angular momentum operator J are expressed as

$$
H_t = -i\sigma_r \frac{\partial}{\partial r} - \frac{i}{r}\sigma_\theta \frac{\partial}{\partial \theta} + t\sigma_3,
\tag{6}
$$

and as

$$
J = \frac{1}{2}\sigma_3 - i\mathbb{1}\frac{\partial}{\partial \theta},
\tag{7}
$$

respectively, where

$$\sigma_r = \begin{pmatrix} 0 & e^{-i\theta} \\ e^{i\theta} & 0 \end{pmatrix}, \qquad \sigma_\theta = \begin{pmatrix} 0 & -ie^{-i\theta} \\ ie^{i\theta} & 0 \end{pmatrix}. \tag{8}$$

On account of the rotational symmetry $[H_t, J] = 0$, the eigenvalue problem $H_t \Phi = E \Phi$ reduces to subproblems in eigenspaces of J. Since the eigenstate Φ_j of J associated with j takes the form

$$\Phi_j(r, \theta) = \begin{pmatrix} e^{i\left(j-\frac{1}{2}\right)\theta} \phi_j^{(-)}(r) \\ e^{i\left(j+\frac{1}{2}\right)\theta} \phi_j^{(+)}(r) \end{pmatrix}, \qquad j \in \left\{ \pm\frac{1}{2}, \pm\frac{3}{2}, \dots \right\}, \tag{9}$$

a straightforward calculation with H_t provides the radial differential equations for unknown functions $\phi_j^{(\pm)}(r)$,

$$-i\frac{d\phi_j^{(+)}}{dr} - \frac{i}{r}\left(j+\frac{1}{2}\right)\phi_j^{(+)} + t\phi_j^{(-)} = E_j \phi_j^{(-)}, \tag{10a}$$

$$-i\frac{d\phi_j^{(-)}}{dr} + \frac{i}{r}\left(j-\frac{1}{2}\right)\phi_j^{(-)} - t\phi_j^{(+)} = E_j \phi_j^{(+)}. \tag{10b}$$

These equations are put together to be brought into second-order Bessel equations;

$$\frac{d^2\phi_j^{(-)}}{dr^2} + \frac{1}{r}\frac{d\phi_j^{(-)}}{dr} + \left(E_j^2 - t^2 - \frac{1}{r^2}\left(j-\frac{1}{2}\right)^2\right)\phi_j^{(-)} = 0, \tag{11a}$$

$$\frac{d^2\phi_j^{(+)}}{dr^2} + \frac{1}{r}\frac{d\phi_j^{(+)}}{dr} + \left(E_j^2 - t^2 - \frac{1}{r^2}\left(j+\frac{1}{2}\right)^2\right)\phi_j^{(+)} = 0. \tag{11b}$$

According to whether $|E_j| > |t|$ or $|E_j| < |t|$, the second-order differential equation becomes the Bessel equation or the modified Bessel equation. The parameter space $\{(E, t)\}$ is divided into four regions (see Fig. 1). To each of four regions, assigned are each type of feasible solution, which are given as follows: For $|E_j| > |t|$, there exist two types of feasible solutions expressed as

$$\Phi_j(r, \theta) = c \begin{pmatrix} \sqrt{E_j + t}\, e^{i\left(j-\frac{1}{2}\right)\theta} J_{j-\frac{1}{2}}(\beta_j r) \\ i\sqrt{E_j - t}\, e^{i\left(j+\frac{1}{2}\right)\theta} J_{j+\frac{1}{2}}(\beta_j r) \end{pmatrix} \qquad \text{for } E_j > 0, \tag{12a}$$

$$\Phi_j(r, \theta) = c' \begin{pmatrix} \sqrt{|E_j + t|}\, e^{i\left(j-\frac{1}{2}\right)\theta} J_{j-\frac{1}{2}}(\beta_j r) \\ -i\sqrt{|E_j - t|}\, e^{i\left(j+\frac{1}{2}\right)\theta} J_{j+\frac{1}{2}}(\beta_j r) \end{pmatrix} \qquad \text{for } E_j < 0, \tag{12b}$$

where J_ν with $\nu = j \pm \frac{1}{2}$ denote the Bessel functions and where

$$\beta_j = \sqrt{E_j^2 - t^2}, \tag{13}$$

Fig. 1. The parameter space is divided into four regions.

and c and c' are complex constants. And for $|E_j| < |t|$, feasible solutions are expressed as

$$\Phi_j(r, \theta) = c \begin{pmatrix} \sqrt{t + E_j} e^{i\left(j - \frac{1}{2}\right)\theta} I_{j-\frac{1}{2}}(\varepsilon_j r) \\ -i\sqrt{t - E_j} e^{i\left(j + \frac{1}{2}\right)\theta} I_{j+\frac{1}{2}}(\varepsilon_j r) \end{pmatrix} \quad \text{for } t > 0, \tag{14a}$$

$$\Phi_j(r, \theta) = c' \begin{pmatrix} \sqrt{|t + E_j|} e^{i\left(j - \frac{1}{2}\right)\theta} I_{j-\frac{1}{2}}(\varepsilon_j r) \\ i\sqrt{|t - E_j|} e^{i\left(j + \frac{1}{2}\right)\theta} I_{j+\frac{1}{2}}(\varepsilon_j r) \end{pmatrix} \quad \text{for } t < 0, \tag{14b}$$

where I_ν with $\nu = j \pm \frac{1}{2}$ denote the modified Bessel functions and where

$$\varepsilon_j = \sqrt{t^2 - E_j^2}, \tag{15}$$

and c and c' are complex constants.

3. Boundary conditions

Though we work with the Dirac equation on $\mathbb{R}^2$, we here deal with boundary conditions in generic form. The Dirac operator on $\mathbb{R}^d$ takes the form

$$H = -i \sum_{k=1}^{d} \gamma_k \nabla_k + \mu \gamma_{d+1}, \quad \nabla_k = \partial/\partial x_k, \tag{16}$$

where μ is a mass parameter taking all real values, and where γ_k are the gamma matrices satisfying

$$\gamma_k \gamma_j + \gamma_j \gamma_k = 2\delta_{jk}, \quad j, k = 1, \ldots, d, \tag{17a}$$

$$\gamma_k \gamma_{d+1} + \gamma_{d+1} \gamma_k = 0, \tag{17b}$$

$$(\gamma_{d+1})^2 = I, \tag{17c}$$

$$(\gamma_\nu)^\dagger = \gamma_\nu, \quad \nu = 1, \dots, d, d+1, \tag{17d}$$

with I denoting the $d \times d$ identity matrix and being used in this section only. The inner products for multi-component functions on a domain $V \subset \mathbb{R}^d$ and on the boundary S of V are defined as usual to be

$$\langle \Phi, \Psi \rangle_V = \int_V \sum \overline{\Phi}_\alpha \Psi_\alpha dV, \qquad \langle \phi, \psi \rangle_S = \int_S \sum \overline{\phi}_\alpha \psi_\alpha dS, \tag{18}$$

respectively, where $\overline{\Phi}_\alpha$ and $\overline{\phi}_\alpha$ denote the complex conjugates of Φ_α and ϕ_α, respectively.

A key idea to finding boundary condition is to apply a kind of Green's formula for the Hamiltonian, which takes the form of the difference between $\langle \Phi, H\Psi \rangle_V$ and $\langle H\Phi, \Psi \rangle_V$. Since $\langle \Phi, \gamma_{d+1}\Psi \rangle = \langle \gamma_{d+1}\Phi, \Psi \rangle$, the difference depends only on the differential operator terms. A straightforward calculation provides

$$\langle \Phi, H\Psi \rangle_V - \langle H\Phi, \Psi \rangle_V = -i \langle \phi, \vec{\gamma} \cdot \vec{n}\, \psi \rangle_S, \tag{19}$$

where $\phi = \Phi|_S$, $\psi = \Psi|_S$ and $\vec{\gamma} \cdot \vec{n} = \sum \gamma_k n_k$ with $\vec{n}$ being the outward unit normal to the boundary surface S.

Boundary conditions should be chosen so that the boundary integral on the right-hand side of (19) may vanish [1]. If we can find such a boundary condition, the Hamiltonian operator becomes a symmetric operator. Furthermore, with some Sobolev conditions, it becomes self-adjoint [6]. We will adopt two boundary conditions, one of which is called the APS (Atiyah–Patodi–Singer) boundary condition [2] and the other the chiral bag boundary condition.

3.1. The APS boundary condition

If we can find a self-adjoint boundary operator B on S such that B has no zero eigenvalue, we obtain the decomposition of the Hilbert space $\mathcal{H}(S)$,

$$\mathcal{H}(S) = \mathcal{H}^{(+)}(S) \oplus \mathcal{H}^{(-)}(S), \tag{20}$$

where $\mathcal{H}^{(\pm)}(S)$ are subspaces such that

$$B|_{\mathcal{H}^{(+)}(S)} > 0, \qquad B|_{\mathcal{H}^{(-)}(S)} < 0. \tag{21}$$

We assume further that the $\vec{\gamma} \cdot \vec{n}$ transforms eigenstates associated with positive eigenvalues of B to those associated with negative ones, and vice versa,

$$(\vec{\gamma} \cdot \vec{n})\mathcal{H}^{(\pm)}(S) = \mathcal{H}^{(\mp)}(S). \tag{22}$$

The APS boundary condition requires that the boundary functions $\phi = \Phi|_S$, $\psi = \Psi|_S$ should belong to the eigenspace associated with either positive or negative eigenvalues.

We have already treated this boundary condition to find eigenvalues for the Dirac equation on a disk of radius R in $\mathbb{R}^2$ [10]. The boundary operator we have used in [10] is given as follows: We denote the restriction of H_t to the circle $r = R$ by

$$A_t = -\frac{i}{R}\sigma_\theta \frac{\partial}{\partial \theta} + t\sigma_3, \tag{23}$$

and define the boundary operator B_t to be

$$B_t = i\sigma_r A_t = \begin{pmatrix} \dfrac{i}{R}\dfrac{\partial}{\partial\theta} & -ite^{-i\theta} \\ ite^{i\theta} & -\dfrac{i}{R}\dfrac{\partial}{\partial\theta} \end{pmatrix}, \tag{24}$$

where $t \neq 0$ in the present section. We note that in the present case the operator $\vec{\gamma}\cdot\vec{n}$ is expressed as σ_r and it satisfies the relation

$$\sigma_r B_t + B_t \sigma_r = \frac{1}{R}\sigma_r. \tag{25}$$

3.2. The chiral bag boundary condition

Taking the operator $\vec{\gamma}\cdot\vec{n}$ into account, one can seek for another boundary condition. According to [1], we decompose spinors into the sum of chiral components,

$$\Phi = \Phi_+ + \Phi_-, \qquad \Phi_\pm := \frac{1}{2}(I \pm \vec{\gamma}\cdot\vec{n})\Phi. \tag{26}$$

It is easy to verify that

$$\vec{\gamma}\cdot\vec{n}\,\Phi_+ = \Phi_+, \qquad \vec{\gamma}\cdot\vec{n}\,\Phi_- = -\Phi_-, \qquad \langle\Psi_+, \Phi_-\rangle = 0. \tag{27}$$

Using these properties, we can put the right-hand side of (19) in the form

$$-i\langle\phi, \vec{\gamma}\cdot\vec{n}\,\psi\rangle_S = -i\langle\phi_+, \psi_+\rangle_S + i\langle\phi_-, \psi_-\rangle_S. \tag{28}$$

If the chiral components $\psi_\pm$ of $\psi = \Psi|_S$ are related by

$$\psi_- = U\gamma_{d+1}\psi_+, \quad \text{or} \quad (I - \vec{\gamma}\cdot\vec{n})\psi = U\gamma_{d+1}(I - \vec{\gamma}\cdot\vec{n})\psi, \tag{29}$$

where U is any unitary operator acting on spinors defined on the boundary and further commutes with $\vec{\gamma}\cdot\vec{n}$, then those components satisfy

$$\langle\phi_-, \psi_-\rangle_S = \langle\phi_+, \psi_+\rangle_S, \tag{30}$$

so that the right-hand side of (28) vanishes. Eq. (29) is called the chiral bag boundary condition.

For the sake of simplicity, we may assume that the unitary operator U is a local one, which is expressed as a finite order matrix acting fiberwise on spinors. A very simple unitary matrix is given by

$$U = e^{2i\arctan e^\lambda}\,I, \tag{31}$$

where the λ is a real parameter. Then, the chiral bag boundary condition (29) reads

$$\vec{\gamma}\cdot\vec{n}\,\psi = -ie^{\lambda\gamma_{d+1}}\gamma_{d+1}\psi. \tag{32}$$

We remark here that from the physical point of view the boundary condition should require that the transverse component of the current vector $\psi^\dagger\vec{\gamma}\psi$ on the boundary must vanish. From (32), one can easily verify that

$$\psi^\dagger(\vec{\gamma}\cdot\vec{n})\psi = 0, \tag{33}$$

which shows that the above-mentioned requirement is indeed satisfied.

4. Eigenstates under the chiral bag boundary condition

For the $2D$ Dirac equation, the chiral bag boundary condition (32) reads

$$\sigma_r \psi = -i e^{\lambda \sigma_3} \sigma_3 \psi, \tag{34}$$

which is written out as

$$\begin{pmatrix} \psi_1 \\ \psi_2 \end{pmatrix} = -i \begin{pmatrix} 0 & -e^{-\lambda} e^{-i\theta} \\ e^{\lambda} e^{i\theta} & 0 \end{pmatrix} \begin{pmatrix} \psi_1 \\ \psi_2 \end{pmatrix}, \tag{35}$$

where ψ_1, ψ_2 denote the boundary values of spinor components. We now apply this condition to the feasible solution obtained in Section 2.

4.1. Edge and regular states

The chiral bag boundary condition (35) gives rise to functional equations for determining eigenvalues. For $|E_j| < |t|$, Eq. (35) applied to (14) with $r = R$ yields

$$\sqrt{\frac{t + E_j}{t - E_j}} I_{j-\frac{1}{2}}(\varepsilon_j R) = e^{-\lambda} I_{j+\frac{1}{2}}(\varepsilon_j R) \quad \text{for } t > 0, \tag{36a}$$

$$-\sqrt{\frac{|t + E_j|}{|t - E_j|}} I_{j-\frac{1}{2}}(\varepsilon_j R) = e^{-\lambda} I_{j+\frac{1}{2}}(\varepsilon_j R) \quad \text{for } t < 0. \tag{36b}$$

For $|E_j| > |t|$, Eqs. (35) and (12) with $r = R$ are put together to yield

$$\sqrt{\frac{E_j + t}{E_j - t}} J_{j-\frac{1}{2}}(\beta_j R) = -e^{-\lambda} J_{j+\frac{1}{2}}(\beta_j R) \quad \text{for } E_j > 0, \tag{37a}$$

$$\sqrt{\frac{|E_j + t|}{|E_j - t|}} J_{j-\frac{1}{2}}(\beta_j R) = e^{-\lambda} J_{j+\frac{1}{2}}(\beta_j R) \quad \text{for } E_j < 0. \tag{37b}$$

As is easily seen, Eq. (36b) admits no solution. We call the eigenstates associated with eigenvalues determined by (36b) and (37) edge and regular states, respectively. Accordingly, there is no edge state for $t < 0$.

These functional equations are numerically solved to give eigenvalues as function of the parameter t, which are shown in Fig. 2.

A remarkable feature observed from the graphs in Fig. 2 is that there exist critical eigenvalues associated with the transition from regular (blue) to edge (red) states, accompanying the variation of the parameter t. We call such states critical (or transient) and study them in the following subsection. Transition from regular to edge states will be dealt with in detail in Section 5. The black lines $E = \pm t$ in Fig. 2 to which critical states belong will be referred to as the boundary lines in Section 7.

Another observation is as to the slope of the edge state eigenvalues as functions of t. The graphs suggest that for sufficiently large t the difference $|E_j(t) - t|$ is large. Then, $\varepsilon_j(t) = \sqrt{t^2 - E_j(t)^2}$ becomes large as well. With this in mind, we apply the asymptotic approximation of the modified Bessel function, $I_{n+\frac{1}{2}}(z) \approx e^z / \sqrt{2\pi z}$, to Eq. (36a). After a simple calculation,
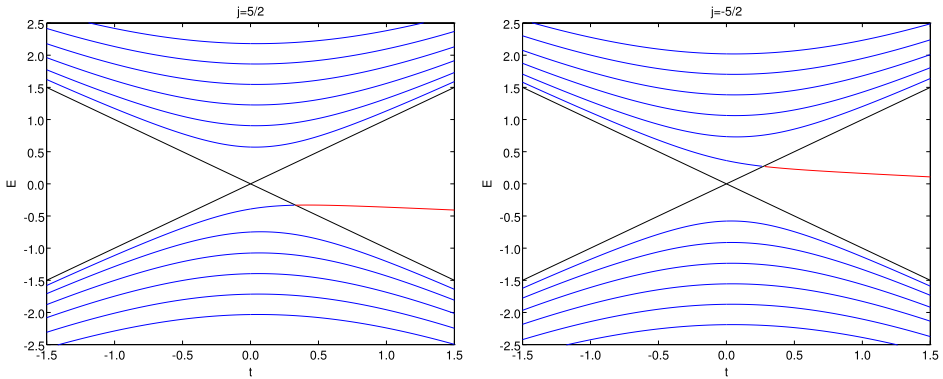
Fig. 2. Eigenvalues of regular (blue) and edge (red) eigenstates with $R = 10$, $\lambda = 0.1$ for $j = 5/2$ (left panel) and for $j = -5/2$ (right panel). Black lines are auxiliary lines $E = \pm t$ separating the regions introduced in Fig. 1. (For interpretation of the references to color in this figure legend, the reader is referred to the web version of this article.)

we find that

$$E_j(t) \approx -t \tanh \lambda. \tag{38}$$

This approximation is so rough that the j-dependence of $E_j(t)$ is lost on the right-hand side of the above equation. However, this approximation explains the reason why the edge state eigenvalues look linear in t. We note in addition that the j-dependence of $E_j(t)$ will be found in Eqs. (49) and (52) for critical eigenstates, in particular.

4.2. Critical states

We will seek for solutions under the condition $|E_j| = |t|$. If $|E_j| = |t|$, Eq. (11) reduces to

$$\frac{d^2\phi_j^{(-)}}{dr^2} + \frac{1}{r}\frac{d\phi_j^{(-)}}{dr} - \frac{1}{r^2}\left(j - \frac{1}{2}\right)^2 \phi_j^{(-)} = 0, \tag{39a}$$

$$\frac{d^2\phi_j^{(+)}}{dr^2} + \frac{1}{r}\frac{d\phi_j^{(+)}}{dr} - \frac{1}{r^2}\left(j + \frac{1}{2}\right)^2 \phi_j^{(+)} = 0. \tag{39b}$$

These equations are easily solved to give, up to constant multiples,

$$\phi_j^{(-)}(r) = r^{j-\frac{1}{2}}, \quad r^{-\left(j-\frac{1}{2}\right)}, \tag{40a}$$

$$\phi_j^{(+)}(r) = r^{j+\frac{1}{2}}, \quad r^{-\left(j+\frac{1}{2}\right)}. \tag{40b}$$

For $j > 0$, taking into account the boundary condition that $\phi_j^{(\pm)}(r)$ are bounded as $r \to 0$, we obtain

$$\phi_j^{(-)}(r) = ar^{j-\frac{1}{2}}, \qquad \phi_j^{(+)}(r) = br^{j+\frac{1}{2}}, \tag{41}$$

where a, b are constants. For $j < 0$, we have, under the same boundary condition,

$$\phi_j^{(-)}(r) = ar^{-\left(j-\frac{1}{2}\right)}, \qquad \phi_j^{(+)}(r) = br^{-\left(j+\frac{1}{2}\right)}. \tag{42}$$

The constants a, b should be related through (10). Eqs. (10) with (41) provide

$$\frac{a}{i\left(j+\frac{1}{2}\right)} = \frac{b}{t}, \qquad E_j = -t. \tag{43}$$

Thus we have obtained feasible solutions

$$\Phi_j(r,\theta) = c \begin{pmatrix} i\left(j+\frac{1}{2}\right)r^{j-\frac{1}{2}}e^{i\left(j-\frac{1}{2}\right)\theta} \\ tr^{j+\frac{1}{2}}e^{i\left(j+\frac{1}{2}\right)\theta} \end{pmatrix}, \qquad E_j = -t \quad \text{for } j > 0. \tag{44}$$

From (10) and (42) in turn, we obtain

$$t = E_j, \qquad \frac{a}{t} = \frac{b}{i\left(j-\frac{1}{2}\right)}, \tag{45}$$

so that feasible solutions of another type take the form

$$\Phi_j(r,\theta) = c' \begin{pmatrix} tr^{-\left(j-\frac{1}{2}\right)}e^{i\left(j-\frac{1}{2}\right)\theta} \\ i\left(j-\frac{1}{2}\right)r^{-\left(j+\frac{1}{2}\right)}e^{i\left(j+\frac{1}{2}\right)\theta} \end{pmatrix}, \qquad E_j = t \quad \text{for } j < 0. \tag{46}$$

We now apply to the above two types of feasible solutions the chiral bag boundary condition (35). For (44), this condition reads

$$\begin{pmatrix} ie^{-\lambda}tR^{j+\frac{1}{2}}e^{i\left(j-\frac{1}{2}\right)\theta} \\ -ie^{\lambda}i\left(j+\frac{1}{2}\right)R^{j-\frac{1}{2}}e^{i\left(j+\frac{1}{2}\right)\theta} \end{pmatrix} = \begin{pmatrix} i\left(j+\frac{1}{2}\right)R^{j-\frac{1}{2}}e^{i\left(j-\frac{1}{2}\right)\theta} \\ tR^{j+\frac{1}{2}}e^{i\left(j+\frac{1}{2}\right)\theta} \end{pmatrix}, \tag{47}$$

which gives

$$t = \frac{e^{\lambda}\left(j+\frac{1}{2}\right)}{R} = -E_j, \quad \text{for } j > 0. \tag{48}$$

Thus, we have found the critical eigenstate, from (44),

$$\Phi_j(r,\theta) = \left(j+\frac{1}{2}\right) \begin{pmatrix} ir^{j-\frac{1}{2}}e^{i\left(j-\frac{1}{2}\right)\theta} \\ \dfrac{e^{\lambda}}{R}r^{j+\frac{1}{2}}e^{i\left(j+\frac{1}{2}\right)\theta} \end{pmatrix}, \qquad E_j^{\text{cri}} = -\frac{e^{\lambda}\left(j+\frac{1}{2}\right)}{R}, \quad \text{for } j > 0. \tag{49}$$

The boundary condition (35) applied to (46) reads in turn

$$\begin{pmatrix} -e^{-\lambda}\left(j-\frac{1}{2}\right)R^{-\left(j+\frac{1}{2}\right)}e^{i\left(j-\frac{1}{2}\right)\theta} \\ -ite^{\lambda}R^{-\left(j-\frac{1}{2}\right)}e^{i\left(j+\frac{1}{2}\right)\theta} \end{pmatrix} = \begin{pmatrix} tR^{-\left(j-\frac{1}{2}\right)}e^{i\left(j-\frac{1}{2}\right)\theta} \\ i\left(j-\frac{1}{2}\right)R^{-\left(j+\frac{1}{2}\right)}e^{i\left(j+\frac{1}{2}\right)\theta} \end{pmatrix}, \tag{50}$$

which provides

$$t = -\frac{e^{-\lambda}\left(j - \frac{1}{2}\right)}{R} = \frac{e^{-\lambda}\left(|j| + \frac{1}{2}\right)}{R} = E_j, \quad \text{for } j < 0. \tag{51}$$

We thus have another critical eigenstate

$$\Phi_j(r, \theta) = \left(j - \frac{1}{2}\right)\begin{pmatrix} -\dfrac{e^{-\lambda}}{R} r^{-\left(j-\frac{1}{2}\right)} e^{i\left(j-\frac{1}{2}\right)\theta} \\ i r^{-\left(j+\frac{1}{2}\right)} e^{i\left(j+\frac{1}{2}\right)\theta} \end{pmatrix}, \tag{52}$$

$$E_j^{\mathrm{cri}} = \frac{e^{-\lambda}\left(|j| + \frac{1}{2}\right)}{R}, \quad \text{for } j < 0.$$

From (48) and (51), we see that there exist critical eigenstates for $t > 0$ only, and that the corresponding critical eigenvalues are positive or negative according as $j < 0$ or $j > 0$.

We note further that the solutions (49) and (52) are described in terms of holomorphic and antiholomorphic functions in $z = re^{i\theta}$, respectively;

$$\Phi_j(r, \theta) = \left(j + \frac{1}{2}\right)\begin{pmatrix} i z^{j-\frac{1}{2}} \\ \dfrac{e^{\lambda}}{R} z^{j+\frac{1}{2}} \end{pmatrix}, \quad j > 0, \tag{53}$$

$$\Phi_j(r, \theta) = \left(j - \frac{1}{2}\right)\begin{pmatrix} -\dfrac{e^{-\lambda}}{R} \bar{z}^{|j|+\frac{1}{2}} \\ i \bar{z}^{|j|-\frac{1}{2}} \end{pmatrix}, \quad j < 0, \tag{54}$$

where $\bar{z}$ denotes the complex conjugate of z.

5. Transition between regular and edge states

So far we have verified that there exist critical states between regular and edge states. We are to show that the transition indeed occurs between regular and edge eigenvalues as well as between regular and edge eigenstates. As is observed from Fig. 2, the transition depends on the sign of j, and hence the study of the transition is accordingly carried out. Before setting out for transition analysis, we introduce two symbols of functions, $J_\nu^P(z)$, $I_\nu^P(z)$, which are the power series factors of the Bessel and the modified Bessel functions, respectively;

$$J_\nu(z) = \left(\frac{z}{2}\right)^\nu J_\nu^P(z), \quad J_\nu^P(z) = \sum_{n=0}^{\infty} \frac{(-1)^n}{n!\,\Gamma(\nu + n + 1)}\left(\frac{z}{2}\right)^{2n}, \tag{55a}$$

$$I_\nu(z) = \left(\frac{z}{2}\right)^\nu I_\nu^P(z), \quad I_\nu^P(z) = \sum_{n=0}^{\infty} \frac{1}{n!\,\Gamma(\nu + n + 1)}\left(\frac{z}{2}\right)^{2n}. \tag{55b}$$

5.1. Eigenvalue transition with $j > 0$

Eq. (36a) determines eigenvalues $E_j(t)$ as a function of t for edge states. We show that the edge state eigenvalues $E_j(t)$ can approach a critical state eigenvalue accompanying a variation in the parameter t. We actually show that $E_j(t)$ has a limit value $E_j(t) \to -t$, a negative critical

eigenvalue. This limiting procedure is allowed in the case of $j > 0$, as is seen from (44) or (49). Using the function I_ν^P defined in (55b), we obtain from (36a)

$$I_{j-\frac{1}{2}}^P(\varepsilon_j R) = \frac{R}{2} e^{-\lambda}(t - E_j) I_{j+\frac{1}{2}}^P(\varepsilon_j R). \tag{56}$$

Since $I_{j-\frac{1}{2}}^P(0) = 1/\Gamma(j + \frac{1}{2})$, $I_{j+\frac{1}{2}}^P(0) = 1/\Gamma(j + \frac{3}{2})$, we obtain, from (56) with $\varepsilon_j(t) = \sqrt{t^2 - E_j(t)^2}$, as $E_j(t) \to -t$,

$$\frac{1}{\Gamma\left(j + \frac{1}{2}\right)} = \frac{R e^{-\lambda} t}{\Gamma\left(j + \frac{3}{2}\right)}, \tag{57}$$

which yields

$$t = \frac{e^\lambda\left(j + \frac{1}{2}\right)}{R}(= -E_j^{\text{cri}}), \tag{58}$$

the same as (48). This means that the edge state eigenvalue $E_j^{\text{edg}}(t)$ approaches the eigenvalue of a critical eigenstate; $E_j^{\text{edg}}(t) \to -\frac{e^\lambda(j+\frac{1}{2})}{R}$, where we have added the superscript "edg" to stress that the eigenvalue $E_j(t)$ is for the edge state.

We proceed to study the transition of regular state eigenvalues to a critical eigenvalue. Since our target eigenvalue is negative (see (58)), we take up (37b) as a functional equation for eigenvalues, Though Eq. (37b) may determine several eigenvalues $E_j(t)$'s of regular states as functions of t, we show that one of $E_j(t)$'s has a limit value $E_j(t) \to -t$, a critical value, like (58). Using the J_ν^P defined in (55a), we obtain from (37b)

$$J_{j-\frac{1}{2}}^P(\beta_j R) = e^{-\lambda}\frac{R}{2}|E_j - t| J_{j+\frac{1}{2}}^P(\beta_j R). \tag{59}$$

Letting $E_j(t) \to -t$ in the above equation with $\beta_j(t) = \sqrt{E_j(t)^2 - t^2}$, we obtain

$$\frac{1}{\Gamma\left(j + \frac{1}{2}\right)} = e^{-\lambda}\frac{tR}{\Gamma\left(j + \frac{3}{2}\right)}, \tag{60}$$

which yields

$$t = \frac{e^\lambda\left(j + \frac{1}{2}\right)}{R}(= -E_j^{\text{cri}}), \tag{61}$$

the same as (58). This means that one of the regular state eigenvalue $E_j^{\text{reg}}(t)$ approaches the eigenvalue of a critical state; $E_j^{\text{reg}}(t) \to -\frac{e^\lambda(j+\frac{1}{2})}{R}$, where we have added the superscript "reg" to indicate that the present eigenvalue $E_j(t)$ is for the regular state. It then turns out that both the regular and the edge state eigenvalues approach the same critical state eigenvalue. Put another way, accompanying the variation in t in the positive direction, the regular state eigenvalue changes into the edge state eigenvalue through a critical state eigenvalue in the case of $j > 0$, where the critical state eigenvalue is negative (see the left panel of Fig. 2).

5.2. *Eigenvalue transition with $j < 0$*

So far we have discussed the transition between regular and edge state eigenvalues accompanying the variation $E_j(t) \to -t$, which occurs if $j > 0$. We turn to the case of $E_j(t) \to t$, which may take place if $j < 0$, as is seen from (46) or (51).

We first deal with the transition from edge state eigenvalues to a critical state eigenvalue. We take up (36a), which is rewritten as

$$\sqrt{\frac{t + E_j}{t - E_j}} I_{-\left(|j|+\frac{1}{2}\right)}(\varepsilon_j R) = e^{-\lambda} I_{-\left(|j|-\frac{1}{2}\right)}(\varepsilon_j R). \tag{62}$$

Since $|j| \pm \frac{1}{2}$ are integers, we use the formula $I_{-n}(z) = I_n(z)$ for n integer to rewrite further the above equation as

$$\sqrt{\frac{t + E_j}{t - E_j}} I_{|j|+\frac{1}{2}}(\varepsilon_j R) = e^{-\lambda} I_{|j|-\frac{1}{2}}(\varepsilon_j R). \tag{63}$$

This determines the eigenvalue $E_j(t)$ as a function of t. In a similar manner to the case of $j > 0$, we obtain, from the above equation,

$$\frac{R}{2}(t + E_j) I^P_{|j|+\frac{1}{2}}(\varepsilon_j R) = e^{-\lambda} I^P_{|j|-\frac{1}{2}}(\varepsilon_j R). \tag{64}$$

Letting $E_j(t) \to t$ in the above equation with $\varepsilon_j = \sqrt{t^2 - E_j(t)^2}$, we obtain

$$\frac{t R}{\Gamma\left(|j| + \frac{3}{2}\right)} = \frac{e^{-\lambda}}{\Gamma\left(|j| + \frac{1}{2}\right)}, \tag{65}$$

which yields

$$t = \frac{e^{-\lambda}\left(|j| + \frac{1}{2}\right)}{R}, \tag{66}$$

the same as (51). This means that the edge state eigenvalue $E_j^{\text{edg}}(t)$ approaches the critical state eigenvalue; $E_j^{\text{edg}}(t) \to \frac{e^{-\lambda}(|j|+\frac{1}{2})}{R}$.

We proceed to the transition from a regular state eigenvalue to the same critical state eigenvalue as above. Since our target is a positive eigenvalue, we pick up (37a) with $j < 0$. As $|j| \pm \frac{1}{2}$ are integers, we use the formula $J_{-n}(z) = (-1)^n J_n(z)$ for n integers. Then, Eq. (37a) is put in the form

$$\sqrt{\frac{E_j + t}{E_j - t}} J_{|j|+\frac{1}{2}}(\beta_j R) = e^{-\lambda} J_{|j|-\frac{1}{2}}(\beta_j R), \tag{67}$$

which determines the eigenvalue $E_j(t)$ as a function of t. By using the symbol $J^P_{|j|\pm\frac{1}{2}}$, this equation is brought into

$$\frac{R}{2}(E_j + t) J^P_{|j|+\frac{1}{2}}(\beta_j R) = e^{-\lambda} J^P_{|j|-\frac{1}{2}}(\beta_j R). \tag{68}$$

Letting $E_j(t) \to t$ in the above equation with $\beta_j = \sqrt{E_j(t)^2 - t^2}$, we obtain

$$\frac{tR}{\Gamma\left(|j| + \frac{3}{2}\right)} = \frac{e^{-\lambda}}{\Gamma\left(|j| + \frac{1}{2}\right)}, \tag{69}$$

which gives

$$t = \frac{e^{-\lambda}\left(|j| + \frac{1}{2}\right)}{R}, \tag{70}$$

the same as (66). This means that the regular state eigenvalues $E_j^{\text{reg}}(t)$ also approach the same critical state eigenvalue; $E_j^{\text{reg}}(t) \to \frac{e^{-\lambda}(|j|+\frac{1}{2})}{R}$. It turns out that accompanying the variation in t regular state eigenvalues change into edge state ones through a critical state eigenvalue in the case of $j < 0$ as well (see the right panel of Fig. 2).

5.3. Eigenstate transition with $j > 0$

We now verify that in correspondence to the transition between edge and regular state eigenvalues, the associated edge and regular eigenstates change indeed into each other through a critical eigenstate. We first show that edge eigenstates associated with the eigenvalue $E_j(t)$ determined by (36a) or (56) approach a critical eigenstate. Taking into account the fact that our target eigenstate is associated with a negative eigenvalue, we start with and arrange (14a) with $E_j(t)$ in question to obtain

$$\begin{pmatrix} \sqrt{t + E_j}\, e^{i\left(j - \frac{1}{2}\right)\theta} I_{j - \frac{1}{2}}(\varepsilon_j r) \\ -i\sqrt{t - E_j}\, e^{i\left(j + \frac{1}{2}\right)\theta} I_{j + \frac{1}{2}}(\varepsilon_j r) \end{pmatrix}$$

$$= \left(\frac{\varepsilon_j}{2}\right)^{j - \frac{1}{2}} \sqrt{t + E_j} \begin{pmatrix} e^{i\left(j - \frac{1}{2}\right)\theta} r^{j - \frac{1}{2}} I_{j - \frac{1}{2}}^P(\varepsilon_j r) \\ -i\dfrac{t - E_j}{2} r^{j + \frac{1}{2}} e^{i\left(j + \frac{1}{2}\right)\theta} I_{j + \frac{1}{2}}^P(\varepsilon_j r) \end{pmatrix}.$$

Deleting, from the right-hand side of the above equation, the scalar factor that depends only on the parameter and vanishes as $E_j(t) \to -t$, we introduce the edge state

$$\tilde{\Phi}_j^{\text{edg}} = \begin{pmatrix} e^{i\left(j - \frac{1}{2}\right)\theta} r^{j - \frac{1}{2}} I_{j + \frac{1}{2}}^P(\varepsilon_j r) \\ -i\dfrac{t - E_j}{2} r^{j + \frac{1}{2}} e^{i\left(j + \frac{1}{2}\right)\theta} I_{j + \frac{1}{2}}^P(\varepsilon_j r) \end{pmatrix}, \tag{71}$$

which remains to be an eigenstate associated with the same eigenvalue $E_j(t)$. When $E_j(t)$ tends to $-t$, the $\tilde{\Phi}_j^{\text{edg}}$ approaches

$$\tilde{\Phi}_j^{\text{edg}} \to \frac{1}{\Gamma\left(j + \frac{1}{2}\right)} \begin{pmatrix} r^{j - \frac{1}{2}} e^{i\left(j - \frac{1}{2}\right)\theta} \\ -i\dfrac{e^{\lambda}}{R} r^{j + \frac{1}{2}} e^{i\left(j + \frac{1}{2}\right)\theta} \end{pmatrix}, \tag{72}$$

where use has been made of (58). The right-hand side is the same as the critical eigenstate (49) within a constant factor.

We show that the regular eigenstate associated with $E_j(t)$ in question changes into a critical eigenstate as well, where $E_j(t)$ is determined by (37b) or (59). Since our target eigenstate has a negative eigenvalue, we start with and arrange (12b) to obtain

$$
\begin{pmatrix}
\sqrt{|E_j + t|}e^{i\left(j-\frac{1}{2}\right)\theta} J_{j-\frac{1}{2}}(\beta_j r) \\
-i\sqrt{|E_j - t|}e^{i\left(j+\frac{1}{2}\right)\theta} J_{j+\frac{1}{2}}(\beta_j r)
\end{pmatrix}
= \left(\frac{\beta_j}{2}\right)^{j-\frac{1}{2}} \sqrt{|E_j + t|}
\begin{pmatrix}
r^{j-\frac{1}{2}}e^{i\left(j-\frac{1}{2}\right)\theta} J^P_{j-\frac{1}{2}}(\beta_j r) \\
-i\dfrac{|E_j - t|}{2}r^{j+\frac{1}{2}}e^{i\left(j+\frac{1}{2}\right)\theta} J^P_{j+\frac{1}{2}}(\beta_j r)
\end{pmatrix}.
$$

In a similar manner to the above, we introduce

$$
\tilde{\Phi}^{\text{reg}}_j =
\begin{pmatrix}
r^{j-\frac{1}{2}}e^{i\left(j-\frac{1}{2}\right)\theta} J^P_{j-\frac{1}{2}}(\beta_j r) \\
-i\dfrac{|E_j - t|}{2}r^{j+\frac{1}{2}}e^{i\left(j+\frac{1}{2}\right)\theta} J^P_{j+\frac{1}{2}}(\beta_j r)
\end{pmatrix},
\tag{73}
$$

which remains an eigenstate associated with the same eigenvalue $E_j(t)$. Letting $E_j(t) \to -t$, we obtain

$$
\tilde{\Phi}^{\text{reg}}_j \to \frac{1}{\Gamma\left(j+\frac{1}{2}\right)}
\begin{pmatrix}
r^{j-\frac{1}{2}}e^{i\left(j-\frac{1}{2}\right)\theta} \\
-i\dfrac{e^{\lambda}}{R}r^{j+\frac{1}{2}}e^{i\left(j+\frac{1}{2}\right)\theta}
\end{pmatrix},
\tag{74}
$$

where we have used (61). The right-hand side is the same as (72), which means that the regular eigenstate $\tilde{\Phi}^{\text{reg}}_j$ approaches the same critical eigenstate as that $\tilde{\Phi}^{\text{edg}}_j$ does. Eqs. (72) and (74) are put together to give the transition in eigenstates, as $E_j(t) \to -t$, in the case of $j > 0$,

$$
\tilde{\Phi}^{\text{reg}}_j \longrightarrow \frac{1}{\Gamma\left(j+\frac{1}{2}\right)}
\begin{pmatrix}
r^{j-\frac{1}{2}}e^{i\left(j-\frac{1}{2}\right)\theta} \\
-i\dfrac{e^{\lambda}}{R}r^{j+\frac{1}{2}}e^{i\left(j+\frac{1}{2}\right)\theta}
\end{pmatrix} \longleftarrow \tilde{\Phi}^{\text{edg}}_j.
\tag{75}
$$

This means that the transition between regular and edge states occurs indeed in accordance with the eigenvalue transition mentioned in Section 5.1.

5.4. Eigenstate transition with $j < 0$

We start with the edge eigenstate (14a) with $j < 0$ and with E_j determined by (36a). By using the symbols $I^P_{|j|\pm\frac{1}{2}}$, Eq. (14a) is arranged as

$$
\begin{pmatrix}
\sqrt{t + E_j}e^{i\left(j-\frac{1}{2}\right)\theta} I_{j-\frac{1}{2}}(\varepsilon_j r) \\
-i\sqrt{t - E_j}e^{i\left(j+\frac{1}{2}\right)\theta} I_{j+\frac{1}{2}}(\varepsilon_j r)
\end{pmatrix}
= \left(\frac{\varepsilon_j}{2}\right)^{|j|-\frac{1}{2}} \sqrt{t - E_j}
\begin{pmatrix}
\dfrac{t + E_j}{2}e^{-i\left(|j|+\frac{1}{2}\right)\theta}r^{|j|+\frac{1}{2}} I^P_{|j|+\frac{1}{2}}(\varepsilon_j r) \\
-ie^{-i\left(|j|-\frac{1}{2}\right)\theta}r^{|j|-\frac{1}{2}} I^P_{|j|-\frac{1}{2}}(\varepsilon_j r)
\end{pmatrix}.
$$

Deleting the scalar factor from the right-hand side of the above equation, we introduce

$$
\tilde{\psi}_j^{\mathrm{egd}} = \begin{pmatrix} \dfrac{t + E_j}{2} e^{-i\left(|j|+\frac{1}{2}\right)\theta} r^{|j|+\frac{1}{2}} I_{|j|+\frac{1}{2}}^P (\varepsilon_j r) \\[2mm] -i e^{-i\left(|j|-\frac{1}{2}\right)\theta} r^{|j|-\frac{1}{2}} I_{|j|-\frac{1}{2}}^P (\varepsilon_j r) \end{pmatrix}, \tag{76}
$$

which remains to be an eigenstate associated with the same eigenvalue. Letting $E_j(t) \to t$ results in

$$
\tilde{\psi}_j^{\mathrm{egd}} \to \frac{1}{\Gamma\left(|j|+\frac{1}{2}\right)} \begin{pmatrix} \dfrac{e^{-\lambda}}{R} e^{-i\left(|j|+\frac{1}{2}\right)\theta} r^{|j|+\frac{1}{2}} \\[2mm] -i e^{-i\left(|j|-\frac{1}{2}\right)\theta} r^{|j|-\frac{1}{2}} \end{pmatrix}. \tag{77}
$$

Since the right-hand side of the above equation is the same as (52) within a constant factor, the edge eigenstate $\tilde{\psi}_j^{\mathrm{edg}}$ is shown to approach a critical eigenstate.

We take up (12a) with $j < 0$ and with E_j determined by (37a) or (68). Using the symbols $J_{|j|\pm\frac{1}{2}}^P$, we rewrite (12a) as

$$
\begin{pmatrix} \sqrt{E_j + t}\, e^{i\left(j-\frac{1}{2}\right)\theta} J_{j-\frac{1}{2}} (\beta_j r) \\[2mm] i\sqrt{E_j - t}\, e^{i\left(j+\frac{1}{2}\right)\theta} J_{j+\frac{1}{2}} (\beta_j r) \end{pmatrix}
$$
$$
= (-1)^{|j|+\frac{1}{2}} \left(\frac{\beta_j}{2}\right)^{|j|-\frac{1}{2}} \sqrt{E_j - t} \begin{pmatrix} \dfrac{E_j + t}{2} e^{-i\left(|j|+\frac{1}{2}\right)\theta} r^{|j|+\frac{1}{2}} J_{|j|+\frac{1}{2}}^P (\beta_j r) \\[2mm] -i e^{-i\left(|j|-\frac{1}{2}\right)\theta} r^{|j|-\frac{1}{2}} J_{|j|-\frac{1}{2}}^P (\beta_j r) \end{pmatrix}.
$$

In a similar manner to the above, we introduce

$$
\tilde{\psi}_j^{\mathrm{reg}} = \begin{pmatrix} \dfrac{E_j + t}{2} e^{-i\left(|j|+\frac{1}{2}\right)\theta} r^{|j|+\frac{1}{2}} J_{|j|+\frac{1}{2}}^P (\beta_j r) \\[2mm] -i e^{-i\left(|j|-\frac{1}{2}\right)\theta} r^{|j|-\frac{1}{2}} J_{|j|-\frac{1}{2}}^P (\beta_j r) \end{pmatrix}, \tag{78}
$$

which remains to be an eigenstate associated with the same eigenvalue. Letting $E_j(t) \to t$, we obtain

$$
\tilde{\psi}_j^{\mathrm{reg}} \to \frac{1}{\Gamma\left(|j|+\frac{1}{2}\right)} \begin{pmatrix} \dfrac{e^{-\lambda}}{R} e^{-i\left(|j|+\frac{1}{2}\right)\theta} r^{|j|+\frac{1}{2}} \\[2mm] -i e^{-i\left(|j|-\frac{1}{2}\right)\theta} r^{|j|-\frac{1}{2}} \end{pmatrix}, \tag{79}
$$

the same as (77). This means that the regular eigenstate $\tilde{\psi}_j^{\mathrm{reg}}$ approaches the critical eigenstate as that $\tilde{\psi}_j^{\mathrm{edg}}$ does. Eqs. (77) and (79) are put together to show that as $E_j(t) \to t$, there occurs the transition, in the case of $j < 0$,

$$
\tilde{\psi}_j^{\mathrm{reg}} \longrightarrow \frac{1}{\Gamma\left(|j|+\frac{1}{2}\right)} \begin{pmatrix} \dfrac{e^{-\lambda}}{R} e^{-i\left(|j|+\frac{1}{2}\right)\theta} r^{|j|+\frac{1}{2}} \\[2mm] -i e^{-i\left(|j|-\frac{1}{2}\right)\theta} r^{|j|-\frac{1}{2}} \end{pmatrix} \longleftarrow \tilde{\psi}_j^{\mathrm{edg}}. \tag{80}
$$

This shows that the transition between regular and edge eigenstates indeed occurs in accordance with the eigenvalue transition proved in Section 5.2.

6. Discrete symmetry

In order to understand the pattern of eigenvalues as functions of t, we try to find discrete symmetries (or pseudo-symmetries) for the operators H_t and J. In view of Fig. 2, it seems that the transformation $(E, j) \mapsto (-E, -j)$ would give a key to the understanding of the pattern in question. We then have to take into account the energy-reflection operation, which is not considered as a symmetry in a strict sense. However, we adopt such an operation as a symmetry in an extended sense. The discrete symmetry used (or misused) in this section is to be understood in the extended sense.

We choose to use the operator $i\sigma_2 K$ with a time-reversal operator in mind, where K denotes the complex conjugation operator. Operating H_t and J with $i\sigma_2 K$, we obtain

$$(i\sigma_2 K)H_t(i\sigma_2 K)^{-1} = H_{-t}, \tag{81a}$$

$$(i\sigma_2 K)J(i\sigma_2 K)^{-1} = -J. \tag{81b}$$

However, Eq. (81a) is not satisfactory for our present purpose. If Eq. (81a) were applicable to our present eigenvalue problem, the eigenvalues as functions of t would be reflection-symmetric with respect to the E-axis. However, this is not the case (see Fig. 2). To resolve this discrepancy, we have to take the chiral bag boundary condition (34) into account simultaneously. Operating (34) with $i\sigma_2 K$, we find that

$$\sigma_r(i\sigma_2 K\psi) = ie^{-\lambda\sigma_3}\sigma_3(i\sigma_2 K\psi). \tag{82}$$

This shows that the boundary condition (34) is not preserved. In fact, the right-hand side undergoes a change in sign and the parameter λ is replaced by $-\lambda$.

Instead of $(i\sigma_2)K$, we take up the operator $\sigma_3(i\sigma_2)K$. Then, we can verify that

$$(\sigma_3(i\sigma_2)K)H_t(\sigma_3(i\sigma_2)K)^{-1} = -H_t, \tag{83a}$$

$$(\sigma_3(i\sigma_2)K)J(\sigma_3(i\sigma_2)K)^{-1} = -J. \tag{83b}$$

We now have to examine how the chiral bag boundary condition (34) transforms under the operator $\sigma_3(i\sigma_2)K$. A straightforward calculation shows that if ψ satisfies (34) then $\tilde{\psi} := \sigma_3(i\sigma_2)K\psi$ satisfies the chiral bag boundary condition with λ replaced by $-\lambda$;

$$\sigma_r\tilde{\psi} = -ie^{-\lambda\sigma_3}\sigma_3\tilde{\psi}. \tag{84}$$

Eqs. (83a), (83b), and (84) are put together to imply that if ψ is an eigenstate associated with the energy and the angular momentum eigenvalues (E, j) under the chiral bag boundary condition with a parameter value λ then $\tilde{\psi} := \sigma_3(i\sigma_2)K\psi$ becomes an eigenstate associated with the energy and the angular momentum eigenvalues $(-E, -j)$ under the chiral bag boundary condition with the parameter value $-\lambda$.

In order to show that this extended symmetry is observed in the pattern of eigenvalues as functions of the parameter t, we give in Fig. 3 numerical solutions of the functional equations (36) and (37). In comparison between the left and the right panels of Fig. 3, we recognize that the pattern admits the symmetry $(E, j, \lambda) \to (-E, -j, -\lambda)$. In fact, if we make the graphs reflected with respect to the t-axis ($E \to -E$) in the left panel ($\lambda < 0$), the resultant graphs coincide with the graphs with solid and dashed curves exchanged ($j \to -j$) in the right panel ($\lambda > 0$).
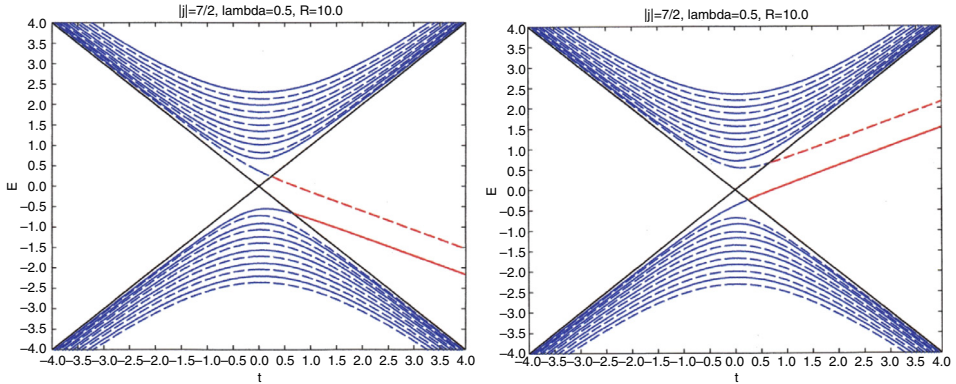
Fig. 3. Eigenvalues of regular (blue) and edge (red) eigenstates with $|j| = \frac{7}{2}$, $R = 10$ and with $\lambda = -0.5$ (left panel) and $\lambda = 0.5$ (right panel). The solid and dashed curves are for $j > 0$ and for $j < 0$, respectively. Black lines are auxiliary lines $E = \pm t$ separating the regions referred to in Fig. 1. (For interpretation of the references to color in this figure legend, the reader is referred to the web version of this article.)
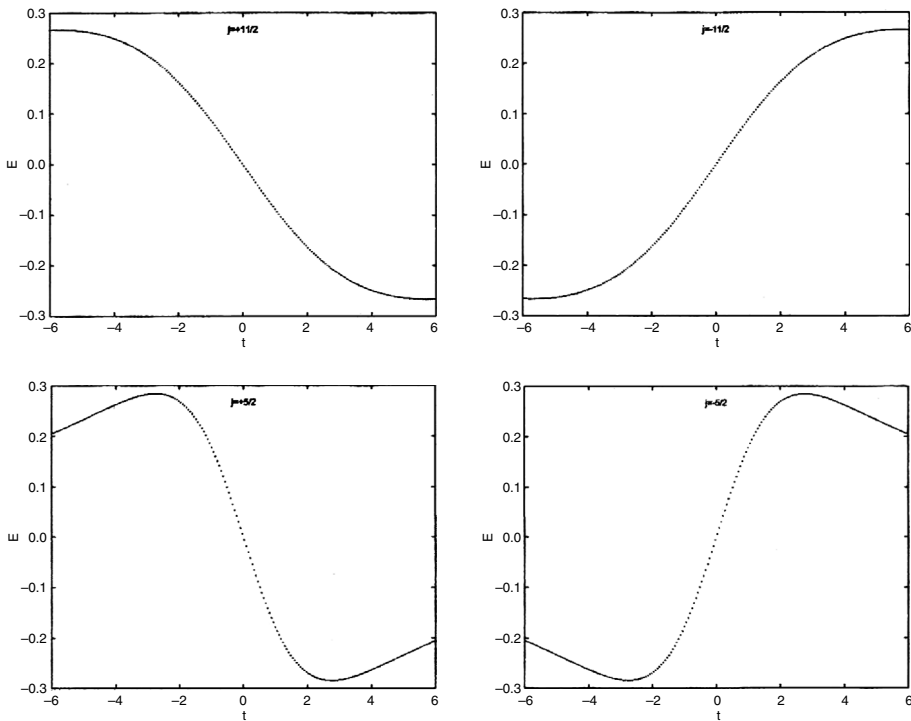

Fig. 4. Edge state eigenvalues as functions of t under the APS boundary condition. Upper and lower left graphs are for $j = 11/2$ and $j = 5/2$, respectively. Upper and lower right graphs are for $j = -11/2$ and $j = -5/2$, respectively.

For the sake of comparison, we quote a figure of edge state eigenvalues obtained under the APS boundary condition [10] (see Fig. 4). Because of the difference in the boundary conditions chosen, the graphs of eigenvalues as functions of t are necessarily different from that obtained

under the chiral bag boundary condition. The different feature can be accounted for by means of the symmetry of the APS boundary condition. For the boundary operator B_t given in (24), we obtain the transformations

$$(i\sigma_2 K) B_t (i\sigma_2 K)^{-1} = B_{-t}, \tag{85}$$

and

$$(\sigma_3(i\sigma_2) K) B_t (\sigma_3(i\sigma_2) K)^{-1} = B_t. \tag{86}$$

From Eqs. (81a), (81b), and (85), we see that if reflected with respect to the E-axis ($t \to -t$) then the graph of the left panel ($j > 0$) of Fig. 4 coincides with that in the right panel ($j < 0$) of Fig. 4. Further, Eqs. (83a), (83b), and (86) are put together to imply that if Φ is an eigenstate associated with (E, j) then $\sigma_3(i\sigma_2) K \Phi$ becomes an eigenstate associated with $(-E, -j)$. Consequently, if the graphs in the left panels of Fig. 4 are reflected with respect to the t-axis ($E \to -E$), then the resultant graphs coincide with those in the right panels.

The present symmetry of the pattern of eigenvalues under the APS boundary condition holds for regular state eigenvalues as well (see Fig. 5 quoted from [10]). We can find further feature of the pattern of the eigenvalues by using these symmetries. Under the APS boundary condition, we operate H_t, J, and B_t with both operators $(i\sigma_2) K$ and $\sigma_3(i\sigma_2) K$ successively. Then, we find that if E is an eigenvalue with j at t then $-E$ is also an eigenvalue with j at $-t$. This implies in particular that the edge eigenvalues as a function of t is odd in t, so that there exists an edge state associated with zero eigenvalue. However, no such symmetry is admitted for the chiral bag boundary condition because of the breaking of the boundary condition under such operations.

7. An extended spectral flow

We have studied the Dirac equation on a two-disk under the chiral bag boundary condition and obtained eigenvalues as functions of the parameter t. Because of the difference between the chiral bag and the APS boundary conditions, the respective eigenvalues as functions of t have different appearances: While there exist zero modes (eigenstates associated with the zero eigenvalue) for the APS boundary condition, there is no such eigenstate for the chiral bag boundary condition. This difference has been explained by means of the discrete symmetry in the last paragraph of the preceding section. A qualitative difference in the band modification between the APS and the chiral bag boundary conditions is described as follows: In the case of the APS boundary condition, the edge state persists to exist at all values of the control parameter except for $t = 0$, but in the case of the chiral bag boundary condition, the transition occurs between regular and edge states, accompanying the variation in the control parameter.

However, there is a common feature between the patterns of eigenvalues for the chiral bag and the APS boundary conditions. In the case of the chiral bag boundary condition, there exists a transient eigenvalue curve which crosses one of the boundary lines $E = \pm t$, depending on whether $j > 0$ or $j < 0$, where the crossing point corresponds to a critical eigenvalue given in (49) or (52), according as $j > 0$ or $j < 0$. In comparison with this, in the case of the APS boundary condition, for each j fixed there exists a transient eigenvalue curve which crosses both the boundary lines $E = \pm t$ at $(E, t) = (0, 0)$ simultaneously. A schematic view of transient eigenvalue curves in the both cases of the chiral bag and the APS boundary conditions is given in Fig. 6. For the both boundary conditions, the dimensionality of the eigenspace of critical states is the same. Furthermore, for the chiral bag boundary condition, the critical state is given, in terms of holomorphic or antiholomorphic functions, by (49) or (52), according as $j > 0$ or $j < 0$. For
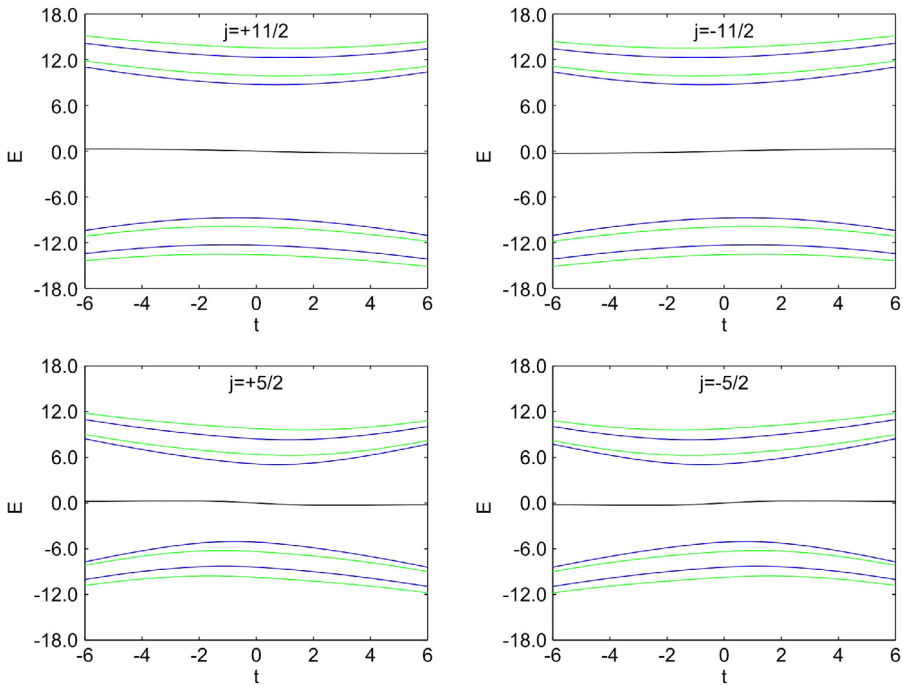
Fig. 5. Regular state eigenvalues as functions of t under the APS boundary condition. Green lines are eigenvalues with the APS boundary conditions which require that the boundary value $\Phi_j(R, \theta)$ should belong to the eigenspaces associated with the negative eigenvalues of the boundary operator B_t. Blue lines are eigenvalues with the APS boundary conditions that $\Phi_j(R, \theta)$ should belong to the eigenspaces associated with the positive eigenvalues of B_t. Black lines are edge state eigenvalues. (For interpretation of the references to color in this figure legend, the reader is referred to the web version of this article.)
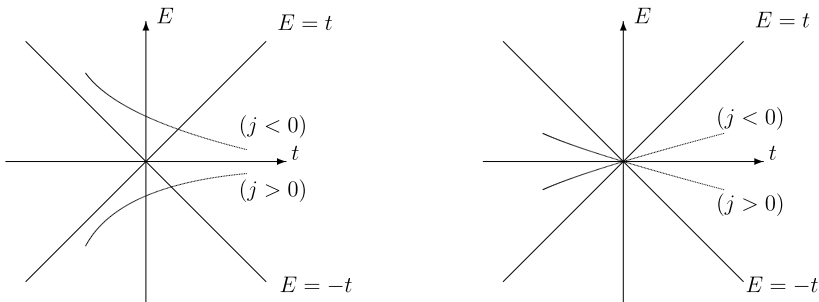
Fig. 6. A schematic view of transient eigenvalue curves, depicted from Figs. 2 and 4. The left and the right panels are for the chiral bag and the APS boundary conditions, respectively. In the left panel, the parameter is chosen as $\lambda = 0$ for simplicity.

the APS boundary condition, the critical state is called a zero mode in [10], which is realized as a special one of (49) or (52) with $E = 0$.

As is well known, the spectral flow for a one-parameter family of operators is the net number of eigenvalues passing through zero in the positive direction as the parameter runs. While the spectral flow is given by $-\mathrm{sgn}(j)$ for the APS boundary condition [10], it is not applicable to

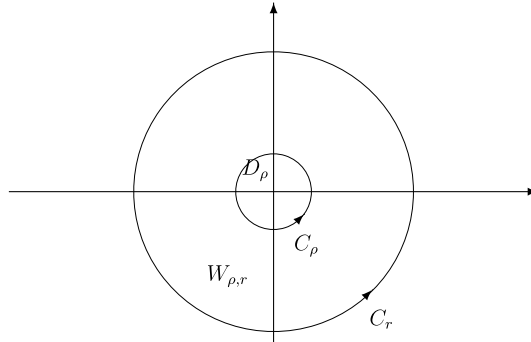the eigenvalues for the chiral bag boundary condition. This is because the crossing of the line $E = 0$ is not associated with any qualitative modification for edge state eigenvalues under the chiral bag boundary condition. However, if we extend the notion of spectral flow to be the net number of eigenvalues crossing the boundary lines $E = \pm t$, we can describe a similar feature of eigenvalues for the chiral bag boundary conditions. If we assign -1 and $+1$ to the crossing of the boundary lines $E = -t$ and $E = t$, respectively, the extended spectral flow for the chiral bag boundary condition is given by $-\mathrm{sgn}(j)$. A reason for the present choice of the assignment of ± 1 is as follows: For $t > 0$, the edge state eigenvalue E_j with $j < 0$ is larger than E_j with $j > 0$ in the both cases of the chiral bag and the APS boundary conditions. The numbers ± 1 are assigned so that the transient eigenvalue curves associated with the higher and the lower eigenvalues for $t > 0$ have $+1$ and -1, respectively, when crossing the boundary lines $E = \pm t$ for the chiral bag boundary condition or the line $E = 0$ for the APS boundary condition.

We remark that since the edge state eigenvalues as functions of the parameter under the APS boundary condition cross the boundary lines $E = \pm t$ simultaneously, the extended spectral flow is zero, which gives no new information for a description of qualitative modification. For the APS boundary condition, we have to employ the usual spectral flow, which counts the net number of the crossing of the line $E = 0$, the mean, $E = \frac{1}{2}(t - t) = 0$, of two boundary lines $E = \pm t$.

8. Delta-Chern in a semi-quantum model

In order to compare band rearrangements for the full quantum mode with those for the semi-quantum model, we make a brief review of a semi-quantum model corresponding to the full quantum Hamiltonian (1), which is given by

$$K_t = \begin{pmatrix} t & k_1 - ik_2 \\ k_1 + ik_2 & -t \end{pmatrix}, \quad \mathbf{k} \in \mathbb{R}^2. \tag{87}$$

The eigenvalues of K_t are

$$\lambda^\pm = \pm\sqrt{k^2 + t^2}, \quad k^2 = k_1^2 + k_2^2. \tag{88}$$

For simplicity, we work with the positive eigenvalue λ^+ only. The normalized eigenvector associated with λ^+ has two complementary expressions as

$$|u_{\mathrm{up}}^+(\mathbf{k})\rangle = \frac{1}{\sqrt{2\lambda^+(\lambda^+ - t)}} \begin{pmatrix} k_1 - ik_2 \\ \lambda^+ - t \end{pmatrix}, \tag{89a}$$

$$|u_{\mathrm{down}}^+(\mathbf{k})\rangle = \frac{1}{\sqrt{2\lambda^+(\lambda^+ + t)}} \begin{pmatrix} \lambda^+ + t \\ k_1 + ik_2 \end{pmatrix}, \tag{89b}$$

where the exceptional points at which the eigenvectors are not defined are present at the origin $\mathbf{k} = 0$; according to whether $t > 0$ or $t < 0$, the origin is the exceptional point for $|u_{\mathrm{up}}^+(\mathbf{k})\rangle$ or for $|u_{\mathrm{down}}^+(\mathbf{k})\rangle$. These two expressions of eigenvectors are related on the intersection of their domains by

$$|u_{\mathrm{up}}^+(\mathbf{k})\rangle = |u_{\mathrm{down}}^+(\mathbf{k})\rangle\varepsilon, \quad \varepsilon = \frac{k_1 - ik_2}{k}. \tag{90}$$

This relation determines the complex line bundle associated with λ^+, which we call the eigen-line bundle and denote by L^+.

Fig. 7. The circles C_ρ and C_r with respective radii ρ and r form the boundary of the annulus $W_{\rho,r}$, and C_ρ is the boundary of the disk D_ρ.

Local connection forms A_{up} and A_{down} for L^+ are defined to be

$$A_{\mathrm{up}} = \langle u_{\mathrm{up}}^+(\boldsymbol{k})|d|u_{\mathrm{up}}^+(\boldsymbol{k})\rangle, \qquad A_{\mathrm{down}} = \langle u_{\mathrm{down}}^+(\boldsymbol{k})|d|u_{\mathrm{down}}^+(\boldsymbol{k})\rangle, \tag{91}$$

respectively. From (90), they are shown to be related by

$$A_{\mathrm{up}} - A_{\mathrm{down}} = \varepsilon^{-1} d\varepsilon. \tag{92}$$

The curvature form F is globally defined on $\mathbb{R}^2$ and evaluated as

$$F = dA_{\mathrm{up}} = dA_{\mathrm{down}} = \frac{i}{2} \frac{t\, dk_1 \wedge dk_2}{(k^2 + t^2)^{3/2}}. \tag{93}$$

The Chern number is formally defined and evaluated, by using (93), as

$$\frac{i}{2\pi} \int_{\mathbb{R}^2} F = -\frac{1}{2}\mathrm{sgn}(t). \tag{94}$$

In what follows, we show that while the formal Chern number (94) is not integer-valued the difference between the formal Chern number for $t > 0$ and that for $t < 0$ takes an integer value, which makes sense as a topological quantity.

For $t > 0$, the origin $\boldsymbol{k} = 0$ is the exceptional point for $|u_{\mathrm{up}}^+(\boldsymbol{k})\rangle$ but not so for $|u_{\mathrm{down}}^+(\boldsymbol{k})\rangle$. With this in mind, we integrate the curvature form, by taking the regions D_ρ and $W_{\rho,r}$ shown in Fig. 7, to obtain

$$\int_{\mathbb{R}^2} F = \int_{D_\rho} dA_{\mathrm{down}} + \lim_{r \to \infty} \int_{W_{\rho,r}} dA_{\mathrm{up}}$$

$$= \int_{C_\rho} A_{\mathrm{down}} + \lim_{r \to \infty} \left(\int_{-C_\rho} A_{\mathrm{up}} + \int_{C_r} A_{\mathrm{up}} \right)$$

$$= -\int_{C_\rho} \varepsilon^{-1} d\varepsilon + \lim_{r \to \infty} \int_{C_r} A_{\mathrm{up}} \quad \text{for } t > 0, \tag{95}$$

where use has been made of the relation (92) and the Stokes theorem. For $t < 0$, the origin is the exceptional point of $|u_{\mathrm{down}}^+(\boldsymbol{k})\rangle$ but not so for $|u_{\mathrm{up}}^+(\boldsymbol{k})\rangle$. A similar calculation to the above

provides

$$\int_{\mathbb{R}^2} F = \int_{C_\rho} \varepsilon^{-1} d\varepsilon + \lim_{r \to \infty} \int_{C_r} A_{\text{down}} \quad \text{for } t < 0. \tag{96}$$

Though Eqs. (95) and (96) contain locally-defined terms, A_{up} and A_{down}, the difference between them may have a characteristic of the eigen-line bundle L^+ depending on t. In fact, one can verify that

$$\frac{i}{2\pi} \int_{\mathbb{R}^2} F\big|_{t>0} - \frac{i}{2\pi} \int_{\mathbb{R}^2} F\big|_{t<0} = \frac{1}{2\pi i} \int_{C_\rho} \varepsilon^{-1} d\varepsilon, \tag{97}$$

where use has been made of the relation (92) and the fact that $\int_{C_r} \varepsilon^{-1} d\varepsilon = \int_{C_\rho} \varepsilon^{-1} d\varepsilon$. Eq. (97) implies that a jump in the formal Chern number accompanying the variation of the parameter t makes sense as a topological invariant, which is a winding number associated with the mapping defined through the transition function; $\varepsilon : C_\rho \to U(1)$. We note further that Eq. (97) holds true for any transition function ε as far as ε is independent of t.

So far we have worked with the jump in the formal Chern number. We now make a comment on the delta-Chern which we have introduced in [9]. We can view the k-plane as the tangent plane to S^2 at the north pole. Then the Hamiltonian (87) is regarded as a linear approximation of some Hamiltonian defined on S^2. In this setting, we have defined a delta-Chern to be a jump which occurs, accompanying the variation of the parameter, in the Chern number of the eigen-line bundle over the unit sphere. According to our definition, the (local) delta-Chern is defined by using the exceptional point of a locally-defined eigenvector and an assigned winding number. In our present case, it is -1 [9,10], the same as the value by (97). Thus, we are allowed to refer to the quantity defined by the left-hand side of (97) as a delta-Chern.

The delta-Chern for the eigen-line bundle L^- associated with the negative eigenvalue λ^- is defined as well, for which the right-hand side of (97) has the opposite sign.

9. Concluding remarks

We have introduced the extended spectral flow and the delta-Chern in Sections 7 and 8, respectively. These two notions characterize the band rearrangements in the full quantum and the semi-quantum models, respectively. In the semi-quantum model, a change in the energy band occurs when the parameter goes through $t = 0$, but in the full quantum model with the chiral bag boundary condition a change occurs at a certain positive value of t, which we refer to as a gap, and view as a kind of quantum effect. For the full quantum model with the APS boundary condition, the gap is zero. Without care for the gap, we may view that the extended or usual spectral flow is in correspondence with the delta-Chern independently of the choice of the boundary conditions, the APS or the chiral bag boundary condition.

So far we have investigated band rearrangements against the control parameter t. We may take another view of band rearrangements of the full quantum model with the total angular momentum j viewed as a discrete parameter. This viewpoint is frequently adopted in the study of molecular spectra.

A schematic view of j-multiplets is given in Fig. 8 at a fixed value of the control parameter. We note that regular state energy levels form two bands represented in black, each of which has the energy levels described by two quantum numbers, j and another, as is observed from Fig. 3. The system of edge states depicted in red in Fig. 8 is assigned by one quantum number j. This
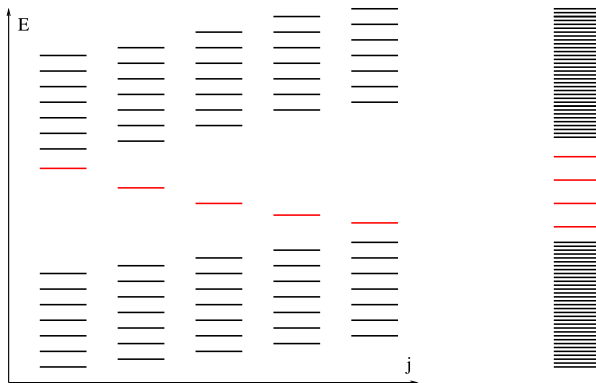
Fig. 8. The left panel shows a system of j-multiplets represented in different columns at a positive value of the control parameter t allowing edge states for several j values. Edge states are shown in red. The right panel describes the same system of energy levels but all multiplets with different j are collected in the same column. (For interpretation of the references to color in this figure legend, the reader is referred to the web version of this article.)
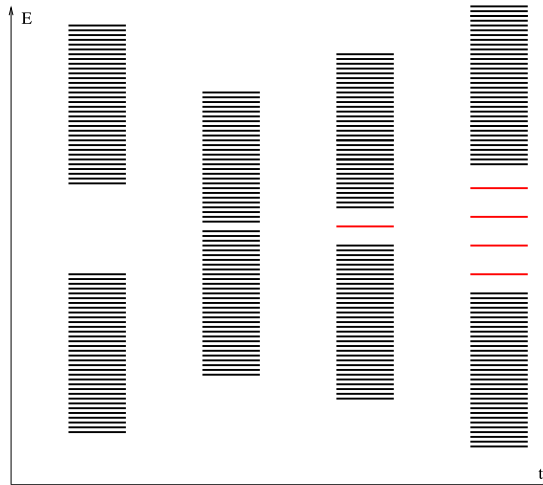

Fig. 9. A schematic evolution of the whole set of levels (all j are treated together) against the control parameter t.

global band structure can be qualitatively characterized as two (two-dimensional or two-quantum number) bands connected by a (one-dimensional or one-quantum number) isthmus.

In Fig. 9, for a generic value of t control parameter, two bands formed by regular state energy levels are shown by respective dense energy level systems with their internal structure described by two quantum numbers (two degrees of freedom). Edge states forming a system of energy levels characterized by one quantum number (one degree of freedom) are shown in red. The scenario corresponding to disappearance/appearance of edge states due to contact between bands is represented along with variation of a control parameter t.

For numerical confirmation of the schematic view of band structures shown in Figs. 8 and 9, we give the numerical evaluation of the pair (j, E) for edge and regular eigenstates in Fig. 10. In particular, the red dots in the right panel of Fig. 10 are exactly given by Eqs. (49) and (52) with the parameter values indicated in Fig. 10.
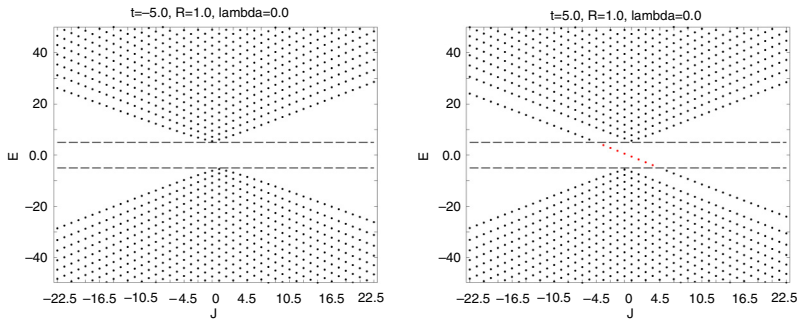
Fig. 10. Eigenvalues of regular (black) and edge (red) eigenstates against j with $R = 1.0$, $\lambda = 0.0$ for $t = -5.0$ (left panel) and for $t = 5.0$ (right panel). The dashed horizontal lines in the left and the right panels correspond to the lines $E = \pm t$ with $t = -5.0$ and $t = 5.0$, respectively. (For interpretation of the references to color in this figure legend, the reader is referred to the web version of this article.)

In conclusion, we add brief remarks on interest in related fields. The Dirac equation on a plane has been treated in topological insulators. The MIT bag (a kind of the chiral bag) boundary condition was used for the massless Dirac equation on a plane [3] in the study of graphene devices. The chiral bag boundary condition is also applied to the Dirac equation for massless spinors on the ball [4]. The half-integer value of the formal Chern number (94) was discussed in relation to the Hall conductivity [13], in which a physical interpretation of the half-integer is given.

Acknowledgments

References

[1] M. Asorey, A.P. Balachandran, J.M. Pérez-Pardo, Edge states: topological insulators, superconductors and QCD chiral bags, J. High Energy Phys. (12) (2013) 073.

[2] M.F. Atiyah, V.K. Patodi, I.M. Singer, Spectral assymetry and Riemannian geometry. I, II, III, Math. Proc. Cambridge Philos. Soc. 77 (1975) 43–69. 78, 405–432 (1975), 79, 71–99 (1976).

[3] C.G. Beneventano, E.M. Santangelo, Boundary conditions in the Dirac approach to graphene devices, Int. J. Mod. Phys. Conf. Ser. 14 (2011) 240.

[4] G. Esposito, K. Kristen, Chiral bag boundary conditions on the ball, Phys. Rev. D 66 (2002) 085014.

[5] F. Faure, B.I. Zhilinskii, Topological Chern indices in molecular spectra, Phys. Rev. Lett. 85 (2000) 960–963.

[6] A. Ibort, J.M. Pérez-Pardo, On the theory of self-adjoint extensions of symmetric operators and its applications to quantum physics, Int. J. Geom. Meth. Mod. Phys. 12 (2015) 1560005.

[7] T. Iwai, B. Zhilinskii, Energy bands: Chern numbers and symmetry, Ann. Physics (NY) 326 (2011) 3013–3066.

[8] T. Iwai, B. Zhilinskii, Rearrangement of energy bands: Chern numbers in the presence of cubic symmetry, Acta Appl. Math. 120 (2012) 153–175.

[9] T. Iwai, B. Zhilinskii, Qualitative feature of the rearrangement of molecular energy spectra from a "wall-crossing" perspective, Phys. Lett. A 377 (2013) 2481–2486.

[10] T. Iwai, B. Zhilinskii, Local description of band rearrangements—Comparison of semi-quantum and full quantum approach, Acta Appl. Math. 137 (2015) 97–121.

[11] V.B. Pavlov-Verevkin, D.A. Sadovskii, B.I. Zhilinskii, On the dynamical meaning of diabolic points, Europhys. Lett. 6 (1988) 573–578.

[12] D.A. Sadovskii, B.I. Zhilinskii, Monodromy, diabolic points, and angular momentum coupling, Phys. Lett. A 256 (1999) 235–244.

[13] H. Watanabe, Y. Hatsugai, H. Aoki, Half-integer contribution to the quantum Hall conductivity from single Dirac cones, Phys. Rev. B 82 (2010) 241403(R).